

LA-UR- 97-1545

CONF-97/111-
RECEIVED

JUL 25 1997

OSTI

Extended pseudo-screen migration with multiple reference velocities

Lian-Jie Huang* and Michael C. Fehler. Los Alamos National Laboratory

Summary

The pseudo-screen propagator is a kind of one-way wave propagation based on the local Born approximation. The problem of the propagator is that it is difficult to calculate the scattered fields when the velocity perturbation is large, not mention the accuracy of the propagator. We develop an extended pseudo-screen propagator by introducing different reference velocities in different regions of a medium to ensure the condition of small perturbation. The exploding reflector data for a 2D slice of the SEG/EAEG 3D salt model is generated by a finite-difference scheme to test the feasibility of the method. The migration result demonstrates that the method can handle severe lateral velocity variations and provides high quality image for complex structures.

Introduction

The split-step Fourier (or phase-screen) propagator has been used for poststack migration (Stoffa *et al.* (1990)), prestack migration (e.g. Huang and Wu, 1996b), and modeling forward and reflected wave propagation (Wu and Huang, 1992; Wu *et al.* 1995). The pseudo-screen propagator is an alternative one-way wave propagator base on the local Born approximation. Wu and Huang (1995) used it for modeling primary reflected waves and Huang and Wu (1996a) applied it to prestack depth migration. Both propagators are based on the assumption of small perturbation. The advantage of the split-step Fourier method is that it is unconditionally stable but the pseudo-screen method is more accurate than the split-step Fourier method. For large velocity perturbations, it is difficult to calculate scattered fields using the pseudo-screen method.

Kessinger (1992) introduced the multiple reference slowness logic of the PSPI migration (Gazdag and Sguazza, 1984) into the split-step Fourier migration in order to handle large lateral velocity variations. By analogy, we introduced multiple reference velocities in the pseudo-screen method. Different reference velocities are chosen in different regions of a medium so that the velocity perturbations are small. The increased computational time of the extended method relative to the original method depends on the number of reference velocities selected. For example, if the average number of reference velocities per depth level is 4, then the CPU time for the proposed method would be ap-

proximately 3 times more than the original method. As in the extended split-step Fourier migration, no interpolation is needed in the proposed method and it can be used to image complex structures with large velocity contrasts. We use a 2D slice of the SEG/EAEG 3D salt model (Amoco, 1995) to test the method and compare the result with those of the original and extended split-step Fourier migrations. Kirchhoff migration, and FX-migration. We show that the quality of the image obtained using the new method is similar to that from the extended split-step Fourier migration but is better than the other methods. The method take about 20-30% more CPU time than the extended split-step Fourier migration with multiple reference velocities but it provides more accurate results for steep dip interfaces than the latter method.

Comparison of the split-step Fourier and pseudo-screen propagators

The split-step Fourier propagator is given by

$$p(x, y, z + \Delta z; \omega) = e^{i\omega \left[\frac{1}{v(x, y, z)} - \frac{1}{v_0(z)} \right] \Delta z} \mathcal{F}^{-1} \left\{ e^{i k_{0z} \Delta z} \mathcal{F} \{ p(x, y, z; \omega) \} \right\}, \quad (1)$$

where $p(x, y, z; \omega)$ is the pressure, ω is the circular frequency, Δz is the vertical extrapolation interval, $v(x, y, z)$ is the velocity of the medium, and $v_0(z)$ is the reference velocity that is chosen as a function of depth. The operators \mathcal{F} and \mathcal{F}^{-1} represent respectively the forward and inverse Fourier transforms over x and y . The vertical component of wavenumber k_{0z} is given by

$$k_{0z} = \sqrt{\frac{\omega^2}{v_0^2(z)} - k_x^2 - k_y^2}, \quad (2)$$

where k_x and k_y are respectively the x - and y -component of wavenumber.

In the pseudo-screen method, the scattered wave field $p_s(x, y, z + \Delta z; \omega)$ is calculated by

$$p_s(x, y, z + \Delta z; \omega) = \frac{i\omega^2}{v_0^2(z)} \left[\frac{v_0(z)}{v(x, y, z)} - 1 \right] \Delta z \mathcal{F}^{-1} \left\{ \frac{1}{\gamma_z} e^{i k_{0z} \Delta z} \mathcal{F} \{ p(x, y, z; \omega) \} \right\}, \quad (3)$$

where γ_z is the modified vertical component of wavenumber given by

$$\gamma_z = \sqrt{\frac{\omega^2}{v_0^2(z)} - (1 + i\eta)^2 (k_x^2 + k_y^2)}. \quad (4)$$

DTIC QUALITY INSPECTED 3

DISTRIBUTION OF THIS DOCUMENT IS UNLIMITED

MASTER

DISCLAIMER

This report was prepared as an account of work sponsored by an agency of the United States Government. Neither the United States Government nor any agency thereof, nor any of their employees, make any warranty, express or implied, or assumes any legal liability or responsibility for the accuracy, completeness, or usefulness of any information, apparatus, product, or process disclosed, or represents that its use would not infringe privately owned rights. Reference herein to any specific commercial product, process, or service by trade name, trademark, manufacturer, or otherwise does not necessarily constitute or imply its endorsement, recommendation, or favoring by the United States Government or any agency thereof. The views and opinions of authors expressed herein do not necessarily state or reflect those of the United States Government or any agency thereof.

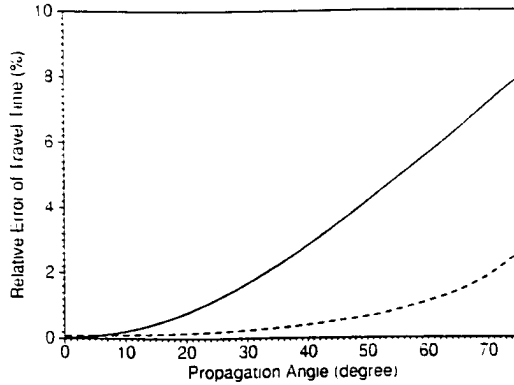


Figure 1: Comparison of relative errors of traveltimes for the split-step Fourier (solid line) and pseudo-screen (dashed line) propagators.

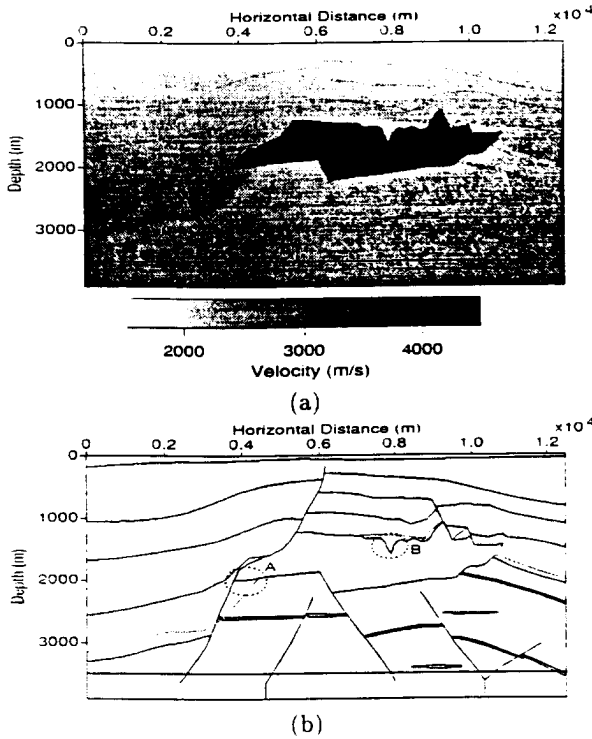


Figure 2: 2D slice of the SEG/EAGE 3D salt model (a) together with its ideal reflectivity (b).

In equation (4), a small real number η is introduced to avoid the numerical singularity when k_{0z} approaches zero (de Hoop and Wu, 1996). The wavefield extrapolation equation for the pseudo-screen method is therefore given by

$$p(x, y, z + \Delta z; \omega) = \mathcal{F}^{-1} \{ e^{i k_{0z} \Delta z} \mathcal{F} \{ p(x, y, z; \omega) \} \} + p_s(x, y, z + \Delta z; \omega). \quad (5)$$

To compare the accuracy between the split-step

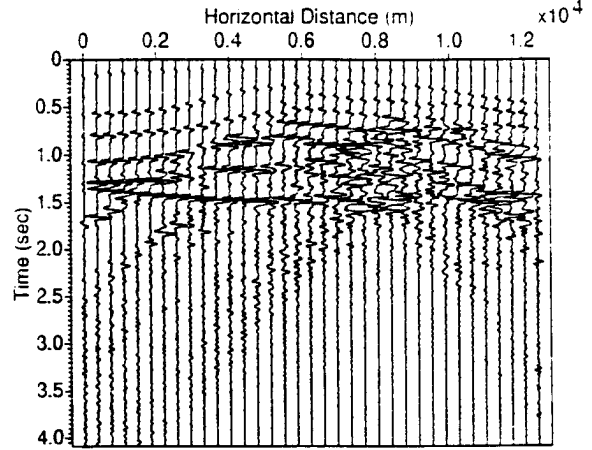


Figure 3: Zero-offset data generated by a FD scheme for the model shown in Figure 2.

Fourier and pseudo-screen propagators. a 2D homogeneous medium defined on a grid 1024×100 was used. The grid spacings along horizontal and vertical directions are both 10m. The velocity of the medium is 4000m/s and a reference velocity of 3636.36m/s was selected. Hence, the whole medium has a relative velocity perturbation 10%. A point source with a Ricker's time history and a dominant frequency 20Hz was introduced at grid site (512,1). Seismograms were recorded at all grid sites from (512,512) to (512,882). The corresponding propagation angles relative to the main propagation direction z -axis range from 0 to 75 degrees. The split-step Fourier and pseudo-screen calculations were respectively made for 512 time steps with a time sample interval 0.004 seconds. The frequency range for both cases is 0.5–60 Hz. Traveltimes picked up from the recorded seismograms were compared with those of seismograms calculated by the analytical solution. The relative errors of traveltime are shown in Figure 1 where the solid line is the result of the split-step Fourier propagator and the dashed line the pseudo-screen propagator. This plot demonstrate that the pseudo-screen propagator is about 5% more accurate than the split-step Fourier propagator when the propagation angle lies between 60–75 degrees.

Extended pseudo-screen propagator with multiple reference velocities

Different reference velocities are selected in the different regions at each depth level so that velocity perturbations in these regions are small enough for the pseudo-screen propagator (for instance 10%). Therefore, equation (3) becomes

$$p_s(x, y, z + \Delta z; \omega) =$$

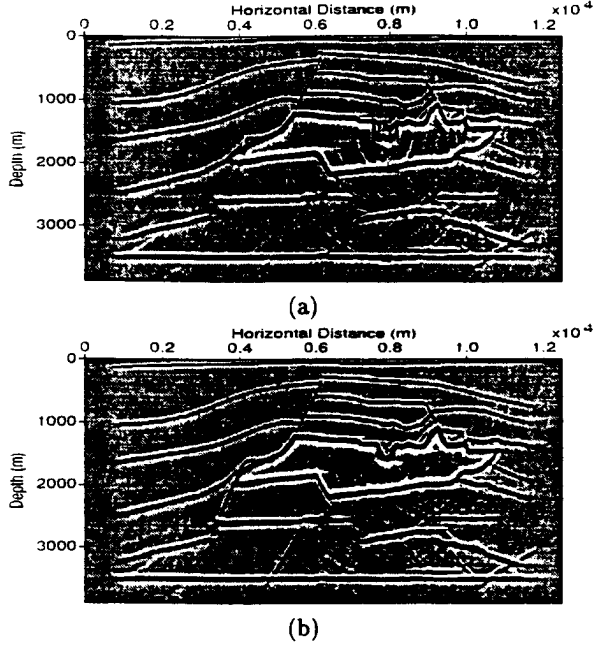


Figure 4: (a) Split-step Fourier migration image. (b) Extended split-step Fourier migration image.

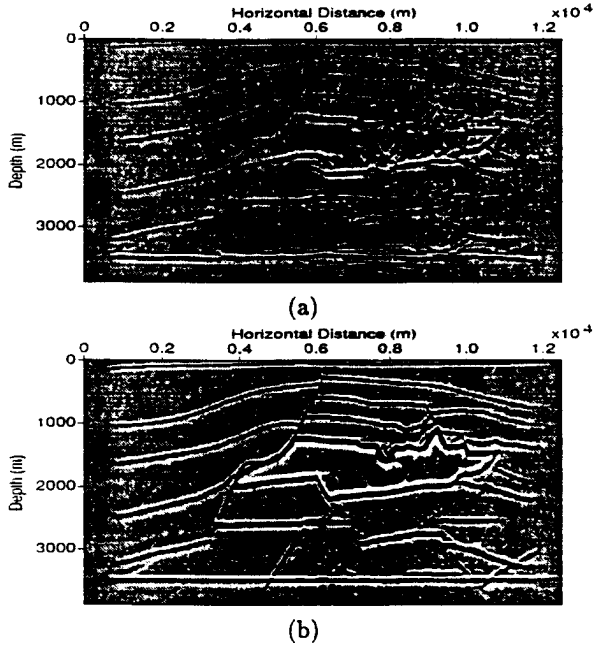


Figure 5: (a) Pseudo-screen migration image. (b) Extended pseudo-screen migration image.

$$\sum_j \delta(M(x, y, z) - v_0^j(z)) \frac{i\omega^2}{v_0^j(z)} \left[\frac{v_0^j(z)}{v(x, y, z)} - 1 \right] \Delta z \\ \mathcal{F}^{-1} \left\{ \frac{1}{\gamma z} e^{i k_0^j z} \Delta z \mathcal{F}\{p(x, y, z; \omega)\} \right\} . \quad (6)$$

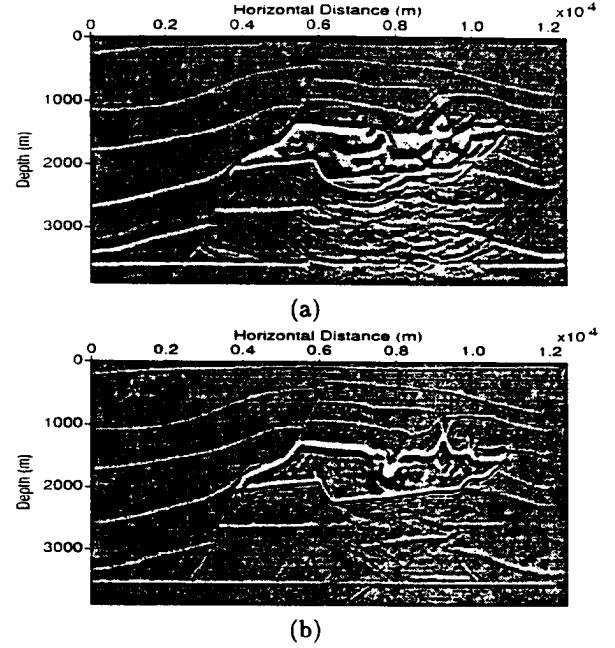


Figure 6: (a) Kirchhoff migration image using first-arrival traveltimes calculated by a FD scheme (From Fei *et al.* 1996). (b) FX-migration image (Amoco, 1995).

where $M(x, y, z)$ is the mapping function between spatial position and reference velocity, and j is the index of reference velocities at each depth level. Equation (6) can also be written as

$$p_s(x, y, z + \Delta z; \omega) = \Pi \left\{ \sum_j \delta(M(x, y, z) - v_0^j(z)) \right. \\ \left. \mathcal{F}^{-1} \left\{ \frac{1}{\gamma z} e^{i k_0^j z} \Delta z \mathcal{F}\{p(x, y, z; \omega)\} \right\} \right\} . \quad (7)$$

where

$$\Pi = \sum_j \delta(M(x, y, z) - v_0^j(z)) \\ \frac{i\omega^2}{v_0^j(z)} \left[\frac{v_0^j(z)}{v(x, y, z)} - 1 \right] \Delta z . \quad (8)$$

Equation (8) can be calculated as soon as reference velocities have been selected, and, therefore, it is more efficient to calculate scattered fields using equation (7) than equation (6). The first term in the right hand side of equation (5) can be written as

$$p_0(x, y, z + \Delta z; \omega) = \sum_j \delta(M(x, y, z) - v_0^j(z)) \\ \mathcal{F}^{-1} \left\{ e^{i k_0^j z} \Delta z \mathcal{F}\{p(x, y, z; \omega)\} \right\} . \quad (9)$$

In equation (7) and (9), the inner fast Fourier transforms are made only once at each depth level. To

reduce alias during migration, a Butterworth filter is applied in the wavenumber domain and a Hann (or raised cosine) taper is used near the boundaries except the upper and lower boundaries of a model.

For migration, the exponential terms and $(i\omega^2)$ in all above equations must be changed to their complex conjugates.

Examples

Figure 2(a) is a 2D slice of the SEG/EAEG 3D salt model provided by Amoco (1995) and Figure 2(b) is its ideal reflectivity. For migration, both grid spacings along horizontal and vertical directions are 12.192m. A finite-difference scheme was used to generate the zero-offset data set (Figure 3) for the 2D salt model. The dominant frequency of the Ricker's time history is 20Hz. The frequency range used in all the following migrations are 5–60Hz. Figure 4 shows migration images by the original and extended split-step Fourier migrations. For the original split-step Fourier migration, the average velocity at each depth level was used as the only reference velocity for that level. The image with multiple reference velocities in Figure 4(b) is much better than Figure 4(a), particularly in the regions A and B where the structures are complex and the lateral velocity variations are large. The pseudo-screen migration image is shown in Figure 5(a) and we can see that there are a lot of artifacts due to the difficulty in the calculations of scattered fields for large velocity contrasts between the salt body and the surrounding media. Figure 5(b) is the migration image from the extended pseudo-screen migration with multiple reference velocities, which clearly images the lower part of the salt body interface, the regions A and B (*cf.* Figure 2(b)), and provides much better images of the interfaces below the salt body than the original pseudo-screen migration. The quality of the image in Figure 5(b) is similar to Figure 4(b) in general. The differences are the details of the images.

For comparison, the corresponding images cut from 3D migration images by the Kirchhoff migration (Fei *et al.* 1996) and FX-migration (Amoco, 1995) are given in Figure 6(a) and (b), respectively. Compare Figure 4(b) and Figure 5(b) with Figure 6(a) and (b), we can see that both multiple reference velocity migrations yield much better images than the Kirchhoff migration, and give clearer images than the FX-migration in the region B (*cf.* Figure 2(b)).

Conclusions

We have developed an extended pseudo-screen migration with multiple reference velocities. Different reference velocities are selected in different regions of a medium so that velocity perturbations are small. No

artifacts associated with multiple reference velocities were observed if the Butterworth filter is applied in the wavenumber domain. The method can be used to image complex structures with severe lateral velocity variations. Computation time increases relative to the original method but could be significantly reduced if an inverse Fourier transform algorithm calculating only the desired part of the output is available.

Acknowledgements

We would like to thank Amoco Production Company for providing the FX-migration image for the SEG/EAEG 3D salt model. Tong Fei and the Gulf of Mexico Subsalt Imaging Project for providing their Kirchhoff migration image. This work is part of the Advanced Computational Technology Initiative. Funding came from the Department of Energy Office of Basic Energy Sciences through contract W-7405-ENG-36.

References

- Amoco Production Company, 1995. Zero-offset data and fx-migration for SEG/EAEG 3D salt model.
- de Hoop, M. V., and Wu, R.-S., 1996. General formulation of screen methods for the scattering of waves in inhomogeneous media: submitted to Wave Motion.
- Fei, T., Fehler, M. C., and Hildebrand, S. T., 1996. Depth migration artifacts associated with first-arrival traveltime: 66th Ann. Internat. Mtg., Soc. Expl. Geophys., Expanded Abstracts, 499–502.
- Gazdag, J., and Sguazzero, P., 1984. Migration of seismic data by phase-shift plus interpolation: Geophysics, **49**, 124–131.
- Huang, L.-J., and Wu, R.-S., 1996a. 3-D prestack depth migration with an acoustic pseudo-screen propagator: in *Mathematical Methods in Geophysical Imaging IV*. S. Hassanzadeh, ed., Proc. SPIE (The International Society for Optical Engineering), **2282**, 40–51.
- Huang, L.-J., and Wu, R.-S., 1996b. Prestack depth migration with acoustic screen propagators: 66th Ann. Internat. Mtg., Soc. Expl. Geophys., Expanded Abstracts, 415–418.
- Kessinger, W., Extended split-step Fourier migration: 62nd Ann. Internat. Mtg., Soc. Expl. Geophys., Expanded Abstracts, 917–920.
- Stoffa, P. L., Fokkema, J. T., de Luna Freire, R. M., and Kessinger, W. P., 1990. Split-step Fourier migration: Geophysics, **55**, 410–421.
- Wu, R.-S., and Huang, L.-J., 1992. Scattered field calculation in heterogeneous media using the phase-screen propagator: 62nd Ann. Internat. Mtg., Soc. Expl. Geophys., Expanded Abstracts, 1289–1292.
- Wu, R.-S., and Huang, L.-J., 1995. Reflected wave modeling in heterogeneous acoustic media using the de Wolf approximation: in S. Hassanzadeh, Editor, *Mathematical Methods in Geophysical Imaging III*. Proc. SPIE **2571**, 176–186.
- Wu, R.-S., Huang, L.-J., and Xie, X.-B., 1995. Backscattered wave calculation using the de Wolf approximation and a phase-screen propagator: 65th Ann. Internat. Mtg., Soc. Expl. Geophys., Expanded Abstracts, 1293–1296.

M97007364



Report Number (14) LA-UR-97-1545

CONE-971111- -

Publ. Date (11) 199707

Sponsor Code (18) DOE/ER, XF

UC Category (19) UC-403, DOE/ER

DOE